Structural Glance Into a Novel Anti-Staphylococcal Peptide

N. B. Iannucci,[1,2] L. M. Curto,[1] F. Albericio,[3,4,5,6] O. Cascone,[1] J. M. Delfino[1]

[1]*Department of Biological Chemistry and Institute of Biochemistry and Biophysics (IQUIFIB), School of Pharmacy and Biochemistry, University of Buenos Aires, Junín 956, C1113AAD Buenos Aires, Argentina*

[2]*Therapeutic Peptides Research and Development Laboratory, Chemo-Romikin, Carlos Villate 5148, B1605AXL, Buenos Aires, Argentina*

[3]*Institute for Research in Biomedicine, Barcelona Science Park, c/Baldiri Reixac 10, 08028, Barcelona, Spain*

[4]*CIBER-BBN, Networking Centre on Bioengineering, Biomaterials and Nanomedicine, Barcelona Science Park, c/Baldiri Reixac 10, 08028, Barcelona, Spain*

[5]*Department of Organic Chemistry, School of Chemistry, University of Barcelona, Martí i Franquès 1-11, 08028, Barcelona, Spain*

[6]*School of Chemistry and Physics, University of KwaZulu-Natal, Westville Campus, University Road, Westville, 4001-Durban, South Africa*

Received 28 March 2013; revised 20 July 2013; accepted 24 July 2013
Published online 27 August 2013 in Wiley Online Library (wileyonlinelibrary.com). DOI 10.1002/bip.22394

ABSTRACT:

Novel antimicrobial peptides are valuable molecules for developing anti-infective drugs to counteract the contemporary spread of microbial drug-resistance. Here we focus on a novel peptide (RKWVWWRNR-NH_2) derived from the fragment 107–115 of the human lysozyme that displays a 20-fold increase in anti-staphylococcal activity. The conformational analysis of this peptide and its interaction with model lipidic phases—as assayed by circular dichroism and fluorescence spectroscopy—show a noteworthy spectral change, which might be related to its anti-staphylococcal activity. The secondary structure of peptide [$K^{108}W^{111}$] 107–115 hLz was dramatically affected through a single substitution at position 111 (Ala by Trp). Therefore, this conformational change might improve the interaction of the novel peptide with the bacterial plasma membrane. These results highlight the role of peptide secondary structure and the distribution of polar/nonpolar residues for the effective interaction of this peptide with the bacterial plasma membrane, a key step for triggering its lethal effect. This knowledge may contribute to the rational design of a new generation of antimicrobial peptides with increased efficacy developed from natural sources by simple screening tools. © *2013 Wiley Periodicals, Inc. Biopolymers (Pept Sci) 102: 49–57, 2014.*

Keywords: human lysozyme; cationic antimicrobial peptides; circular dichroism; fluorescence; conformation; phospholipid detergent micelles

Correspondence to: N. B. Iannucci; e-mail: iannucci@ffyb.uba.ar or J. M. Delfino; e-mail: delfino@qb.ffyb.uba.ar
Contract grant sponsor: CONICET
Contract grant number: PIP 1936, Argentina
Contract grant sponsor: CICYT
Contract grant number: CTQ2012-30930, Spain
© 2013 Wiley Periodicals, Inc.

This article was originally published online as an accepted preprint. The "Published Online" date corresponds to the preprint version. You can request a copy of the preprint by emailing the Biopolymers editorial office at biopolymers@wiley.com

INTRODUCTION

Antimicrobial peptides (AMPs) integrate the native non-specific defense barrier against infections. AMPs are produced at a low metabolic cost by almost all living organisms, especially in microbe-exposed tissues.[1–3] Cationic AMPs (CAMPs) are

typically short peptides with an amphiphilic balance represented by the presence of positively charged and hydrophobic amino acids. Size, sequence, charge, conformation, secondary structure, hydrophobicity, and amphipathicity constitute determining features for the activity and specificity of AMPs. In an attempt to find a meaningful correlation between these features and the activity of a group of CAMPs, Wang et al.[4] introduced the expression membrane perturbation potential, defined by interfacial hydrophobic patches bordered by basic residues.

Activity is usually mediated by direct interaction with the microbial plasma membrane, causing disruption and/or pore generation. The disruption of the microbial plasma membrane is the lethal mechanism exerted by most CAMPs and this process is accomplished in a dual manner, namely by membrane binding and membrane insertion/permeation, related to the charge and the hydrophobicity of the peptide, and its capacity to partition in membranes, respectively.[5] The selectivity of CAMPs for microbial cells over eukaryotic ones is due to the predominant proportion of negatively charged lipids on the surface of the microbial plasma membrane.

CAMPs membrane targeting implies unusual drug-resistance generation. Over the past decades, the emergence of resistance to microbial drugs has become a major health concern, calling into action international health authorities like the Infectious Diseases Society of America.[6] In this regard, biotechnology and small pharmaceutical firms have taken up the challenge of antimicrobial drug development.[7] Original and cost-effective screening approaches for the discovery of new anti-infective drugs are well-regarded by these industries in order to dispel the drug-resistance threat with a minimum investment of venture capital.[8] CAMPs are inspiring molecules for the rational design of new antibiotic compounds as discrete modifications can be introduced into their sequences, thus also addressing the exhaustion of natural sources.

In our previous work, we introduced a new peptide derived from the 107–115 human lysozyme fragment (107-115 hLz) exhibiting a 4- and 20-fold increase in antimicrobial activity against *Escherichia coli* ATCC 25922 and *Staphylococcus aureus* ATCC 29213, respectively.[9] This fragment was selected from the helical hairpin domain of the human lysozyme because it showed stronger bactericidal activity than other fragments and the entire enzyme against a repertoire of microorganisms.[10] The novel analog was developed by a straightforward approach involving the sequential substitution of two Ala residues in the lead peptide by antimicrobial activity-linked amino acids. Antibacterial activity was determined by microdilution assays. Peptide safety was assessed by hemolytic activity, resulting significant at 10-fold its minimal anti-staphylococcal concentration. This new peptide was called [$K^{108}W^{111}$] 107-115 hLz and was selected in a two-round screening from 16 analogs substituted at positions 108 and 111 as described previously.[9] All positively charged and hydrophobic amino acids were included in the screening as antimicrobial-linked amino acids, because of their potential contribution to the amphiphilic balance of the resultant peptides; a feature proposed to be responsible for peptide interaction with microbial membranes.[11] The antimicrobial activity against a drug-resistant strain, methicillin-resistant *Staphylococcus aureus* (*MRSA*) ATCC 43300, was also determined. The 20-fold increase in anti-staphylococcal activity of the novel peptide with respect to the lead was conserved.[12] This result is particularly relevant as regards the striking increase in the incidence of *MRSA* in recent decades.

107	115	
RAWVAWRNR-NH_2		107-115 hLz
RKWVWWRNR-NH_2		[$K^{108}W^{111}$] 107-115 hLz

SCHEME 1 Sequence alignment of 107-115 hLz and [$K^{108}W^{111}$] 107-115 hLz.

The sequences of peptides 107-115 hLz and [$K^{108}W^{111}$] 107-115 hLz are compared in Scheme 1.

This novel peptide interacts in a distinct manner with synthetic membranes composed by staphylococcal-isolated lipids, and saturated phosphatidyl cholines (DMPC) and phosphatidyl ethanolamines (DMPE) when compared with the lead peptide.[13] In order to further understand the structure-activity relationship (SAR) of this peptide, suitable methods for analyzing the secondary structure and its interaction with membrane-mimicking environments were carried out by circular dichroism (CD) and fluorescence spectroscopy. Membrane mimicry was achieved by experiments in the presence of 2,2,2 trifluoroethanol (TFE), a secondary structure-inducing co-solvent, and lipid:detergent micelles, including DMPC or a DMPC/DMPA mixture. With the aim to elucidate a potential correlation between hydrophobicity, amphipaticity, structural conformation and anti-staphylococcal activity, we performed a comparative analysis including two analogs ([N^{108}] 107-115 hLz and [K^{108}] 107-115 hLz).

MATERIALS AND METHODS

Chemicals

Rink-amide resin, Fmoc amino acids, coupling reagents and solvents for peptide synthesis were from Applied Biosystems (Foster City, CA). Solvents for peptide purification were of HPLC grade and were supplied by Tedia Company Inc. (Fairfield, OH). C12E10 and TFE were purchased from Sigma-Aldrich (St. Louis, MO). DMPC and DMPA were from Avanti Polar Lipids, Inc. (Alabaster, AL).

Peptide Synthesis

Peptides were obtained in an ABI 433A Synthesizer (Applied Biosystems, Foster City, CA) using N^{α}-Fmoc protection, following the Fast-Moc 0.10 mmol protocol. Peptides were deprotected and cleaved

Table I Antimicrobial Peptide 107-115 hLz and Its Analogs

Peptide	Sequence	Experimental (Theoretical) MW	Net Charge
107-115 hLz	RAWVAWRNR-NH_2	1213.48 (1213.40)	+4
[N^{108}] 107-115 hLz	R**N**WVAWRNR-NH_2	1256.49 (1256.42)	+4
[K^{108}] 107-115 hLz	R**K**WVAWRNR-NH_2	1270.56 (1270.49)	+5
[$K^{108}W^{111}$] 107-115 hLz	R**K**WV**W**WRNR-NH_2	1385.63 (1385.63)	+5

Ala-substitutions are in bold.

from the resin using a TFA/H_2O/TIS (95:2.5:2.5) solution for 3 h at room temperature.

Peptide Purification

Peptides were purified by RP-HPLC on an Ultrasphere ODS C-18 column (Beckman Instruments, Palo Alto, CA) using a linear gradient of 10–55% acetonitrile in water containing 0.05% TFA.

Peptide Characterization

Peptides were identified by ESI-MS in a LCQ-Duo (ion trap) mass spectrometer (Thermo Fisher, San José, CA). Samples were introduced from a Surveyor pump (Thermo Fisher) in a 40 µL/min solvent flow. Peptide analysis was performed by full Scan 200–2000 amu.

Theoretical molecular weights were calculated with the Protparam tool from the Expasy server: http://www.expasy.org/tools/protparam.html.

Physicochemical prediction of the behavior of each peptide was carried out by calculating the mean hydrophobicity. Amidation at the C-terminal end was not explicitly considered. For this purpose, the Eisenberg consensus scale was used.[14]

Peptide Quantification

Stock solutions were prepared by dissolving the peptides in water. The concentration was determined by UV absorption at 280 nm using their theoretical extinction coefficients: 11,100 M^{-1} cm^{-1} for peptides 107-115 hLZ, [N^{108}] 107-115 hLz, and [K^{108}] 107-115 hLz; and 16650 M^{-1} cm^{-1} for peptide [$K^{108}W^{111}$] 107-115 hLz. Peptides were diluted to a final concentration of 0.11–0.15 mg/mL either in water, PBS (20 m*M* phosphates buffer, 150 m*M* NaCl, pH 7.0), or PBS containing TFE, DMPC, or DMPC/DMPA micelles.

Micelle Preparation

Mixed micelles of phospholipid (DMPC or a DMPC/DMPA mixture) and the nonionic detergent (C12E10) were used in this study. These preparations minimize light-scattering in samples intended for optical spectroscopy. C12E10 does not absorb light in the UV region. A thin dry film of phospholipid:detergent was obtained after evaporation of a chloroform solution of the components in a round-bottomed flask. This procedure was carried out under a nitrogen stream with continuous shaking in a warm water bath. Traces of solvent were eliminated under high vacuum overnight. Lipid films were hydrated in water or PBS for 1 h and then suspended by vortexing with glass beads during 10–15 min. The resultant milky suspension was finally sonicated for 30 min in a bath-type sonicator.

Circular Dichroism Spectroscopy

CD spectra were recorded on a Jasco J-810 spectropolarimeter. Data in the far-UV (200–250 nm) region were collected at 25°C using a 1-mm path cuvette. The scan-speed used was 20 nm min^{-1} with a time constant of 1 s. Each spectrum was measured at least three times, and data were averaged to reduce noise. Molar ellipticity was calculated as described elsewhere.[15]

Fluorescence Measurements

Fluorescence measurements were performed in a Jasco FP-6500 spectrofluorometer equipped with a thermostated cell at 25°C. A 3-mm path cuvette sealed with a Teflon cap was used. The excitation wavelength was 295 nm, and emission was collected in the range 310–410 nm. The excitation and emission monochromator slit widths were both set at 4 nm. For each spectrum, the total integrated intensity and the position of the maximum wavelength of fluorescence emission (λ_{max}) were the parameters used for further analysis.

Table II Characterization of Peptide 107-115 hLz and Its Analogs

		MIC (μM)				
Peptide	Inhibition Power (%)	*S. aureus* ATCC 29213	*MRSA* ATCC 43300	*E. coli* ATCC 25922	Haemolysis (%)	Mean Hydrophobicity<H>
107-115 hLz	49	206	412	412	2.0	0.301
[N^{108}] 107-115 hLz	10	ND	ND	ND	ND	0.200
[K^{108}] 107-115 hLz	98	49	ND	98	3.2	0.157
[$K^{108}W^{111}$] 107-115 hLz	100	11	22	90	5.4	0.372

The inhibition power against *S. aureus* ATCC 29213 at 100 μg/mL, the minimum inhibition concentration (MIC) against different bacterial strains, the hemolytic activity against human red blood cells at 50 μg/mL and mean hydrophobicity are shown. For experimental details see Refs. 9 and 12.

RESULTS AND DISCUSSION

Biological Activity and Physicochemical Features of Peptides

Tables I and II summarize the sequences of peptide 107-115 hLz and its analogs, comparing their experimental and theoretical molecular weights (see Materials and Methods), their net charge and relevant features related to their activity. Two peptides in which position 108 was substituted were included in this study for the sake of comparison: [N^{108}] 107-115 hLz and [K^{108}] 107-115 hLz. The former serves as a model exhibiting reduced inhibition power and the latter highlights the beneficial role of an additional positive charge near the *N* terminus (Table II). The combination of this positive charge with an extra hydrophobic aromatic residue (Trp) at position 111, as in [$K^{108}W^{111}$] 107-115 hLz, maximizes the anti-staphylococcal effect. With respect to selectivity, while the lead peptide and [K^{108}]107-115 hLz showed a 2-fold increase in activity against Gram-positive as compared to Gram-negative organisms, the novel peptide showed markedly enhanced activity against Staphylococci (8-fold). However, it is noteworthy that upon substituting Ala by Trp at position 111, the effectiveness of antimicrobial activity against the Gram-negative organism did not change. Furthermore, [$K^{108}W^{111}$] 107-115 hLz demonstrated a 20-fold increased anti-staphylococcal effect against the methicillin-resistant strain ATCC 43300.

A comparative analysis of peptide 107-115 hLz and its analogs produced some interesting results. For peptide [N^{108}] 107-115 hLz, the substitution with a polar noncharged residue at this position reduced its mean hydrophobicity and inhibition power. In contrast, for peptide [K^{108}] 107-115 hLz, although this substitution reduced the mean hydrophobicity to a greater extent, the inhibition power doubled that of the lead peptide. Correspondingly, the MIC value was 4-fold lower. For this peptide, the positive charge of Lys^{108} played a major role for the enhanced anti-staphylococcal activity and for determining its specificity for negative over zwitterionic membranes, like those of erythrocytes, as demonstrated by its lower hemolytic activity.[9] The increase in the overall positive charge of peptides might enhance their affinity for negative membranes.[11] Finally, for peptide [$K^{108}W^{111}$] 107-115 hLz, the two substitutions resulted in a proper combination of positive net charge and hydrophobicity, thus enhancing its anti-staphylococcal effect. The predicted mean hydrophobicity of 107-115 hLz and [$K^{108}W^{111}$] 107-115 hLz correlated with their experimental hydrophobicity, as measured by their retention times in a C18 HPLC column: 18.3 and 21.1 min, respectively. However, although overall hydrophobicity is the main driving force dictating peptide binding to the apolar matrix, secondary structure propensity — bringing about a change in polar/non-polar character along the peptide — is also able to tune this process.[16] These results are consistent with previous observations on the enhanced interaction of [$K^{108}W^{111}$] 107-115 hLz with lipidic monolayers.[13] Both pieces of evidence point to an increased partition coefficient in hydrophobic phases, which is postulated to be a key factor governing the increased biological potency of AMPs.

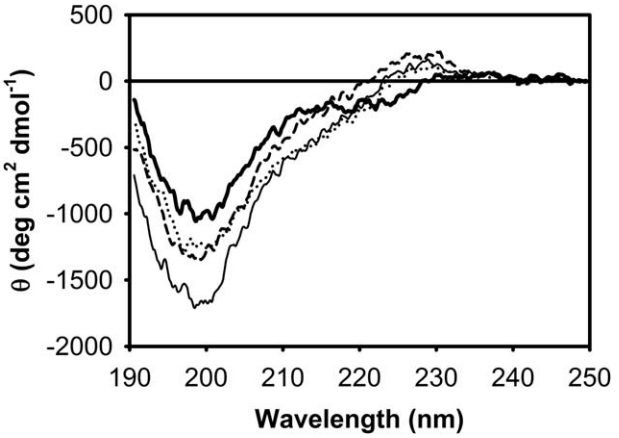

FIGURE 1 Far UV-CD spectra of peptides in water. 107-115 hLz (—), [N^{108}] 107-115 hLz (· · · ·), [K^{108}] 107-115 (– –) and [$K^{108}W^{111}$] 107-115 hLz (▬).

Circular Dichroism Spectroscopy

CD spectroscopy is a powerful and simple tool through which to study the SAR of peptides and proteins. Interaction assays performed in the presence of lipidic (neutral or charged) micelles or vesicles shed light on peptide behavior in a membranous environment. Furthermore, this tool meets the analytical capacity of small pharmaceutical industries to assess the structural features of newly developed AMPs. Many authors have elucidated SAR aspects of AMPs by CD-based studies.[17–19] The overall shape of CD spectra reveals that the four peptides adopted a predominant random coil conformation in water (Figure 1). Interestingly, the spectrum of [$K^{108}W^{111}$] 107-115 hLz shows two distinctive features: (i) a lower minimum at ~200 nm, and (ii) a shallow valley near 220 nm. The significantly lower intensity of the ~200 nm dichroic band (~40% with respect to the lead peptide) points to a decreased content of disordered structure. Consistent with this observation, the incipient 222-nm band might be attributable to the extra aromatic contribution of Trp^{111} in an ordered environment.

TFE is widely recognized as a useful co-solvent to assess the secondary structure propensity of peptides and proteins. However, its general action is to promote α-helix and β-hairpin secondary structure formation in peptides.[20] Despite the short size (9 amino acids) of the peptides, in order to analyze their

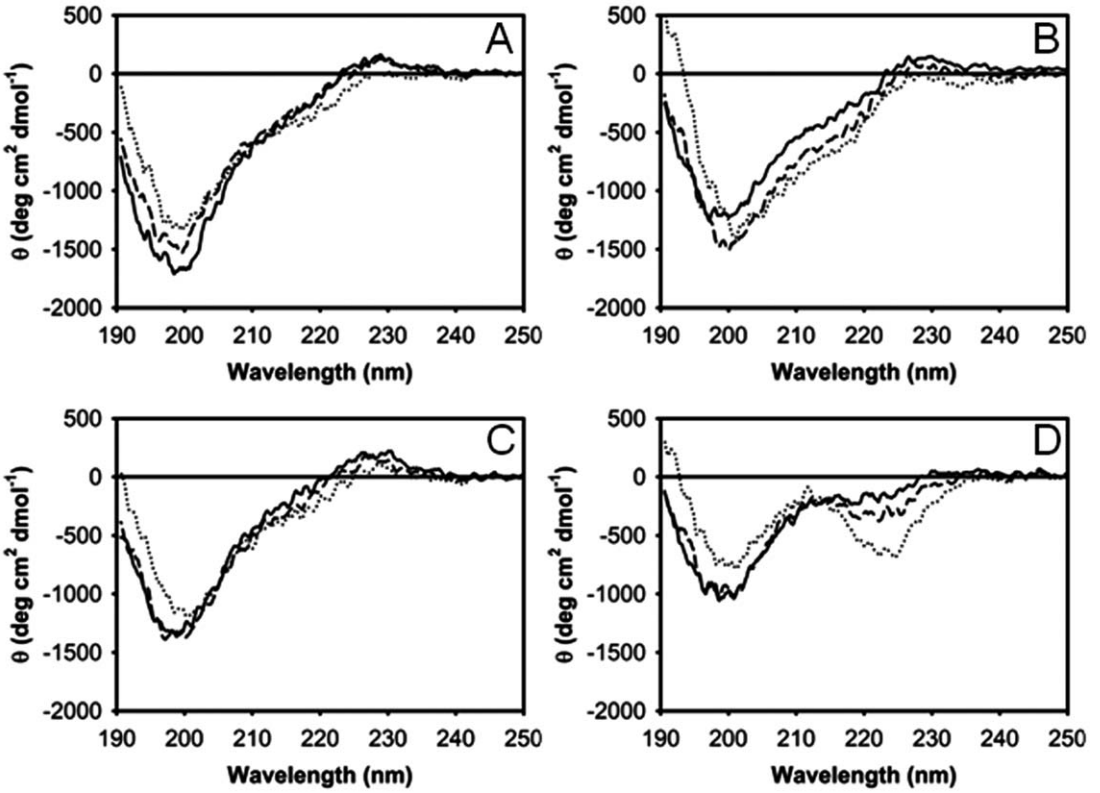

FIGURE 2 Far UV-CD spectra of 107-115 hLz (A), [N^{108}] 107-115 hLz (B) [K^{108}] 107-115 hLz (C) and [K^{108}W^{111}] 107-115 hLz (D) at increasing aqueous TFE concentrations: 0 —, 10 – – – and 25%.... v/v.

structural behavior, we measured the far UV-CD spectra after challenging the molecules with this co-solvent. For peptides 107-115 hLz, [N^{108}] 107-115 hLz, and [K^{108}] 107-115 hLz, the overall pattern of the far UV-CD bands was maintained at all the TFE concentrations assayed (Figures 2A–2C). At the highest TFE concentration, this cosolvent caused a 25% reduction in the magnitude of the ~200-nm band for [K^{108}W^{111}] 107-115 hLz and for the lead peptide (Figures 2A and 2D). It should be noted that for the novel peptide this band was about 60% less intense than that of the lead, an observation indicative of a higher defined structural content for [K^{108}W^{111}] 107-115 hLz. At variance with this behavior, this effect was less evident for [N^{108}] 107-115 hLz and [K^{108}] 107-115 hLz. Furthermore, peptide [K^{108}W^{111}] 107-115 hLz showed a distinct trend toward the enhancement of the 222-nm band at increasing TFE concentrations, a feature that clearly differed from the lead peptide (Figure 2D). The evolution of this signal is plotted in Figure 3. Peptide [K^{108}W^{111}] 107-115 hLz exhibited a steeper slope than the rest, implying greater sensitivity toward the co-solvent.

The canonical CD-spectrum bands for α-helical peptides were not present for [K^{108}W^{111}] 107-115 hLz, as expected due to its short size. In addition, its high Trp-content might complicate interpretation of the CD-spectrum. As revealed by the differences in spectra between [K^{108}W^{111}] 107-115 hLz and [K^{108}] 107-115 hLz (Figure 4), two distinctive features were

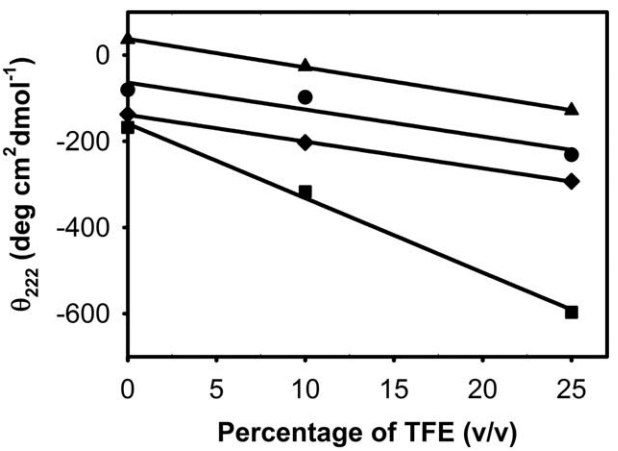

FIGURE 3 Evolution of ellipticity at 222 nm for peptides 107-115 hLz (●), [N^{108}] 107-115 hLz (◆) [K^{108}] 107-115 hLz (▲) and [K^{108}W^{111}] 107-115 hLz (■) as a function of aqueous TFE concentration.

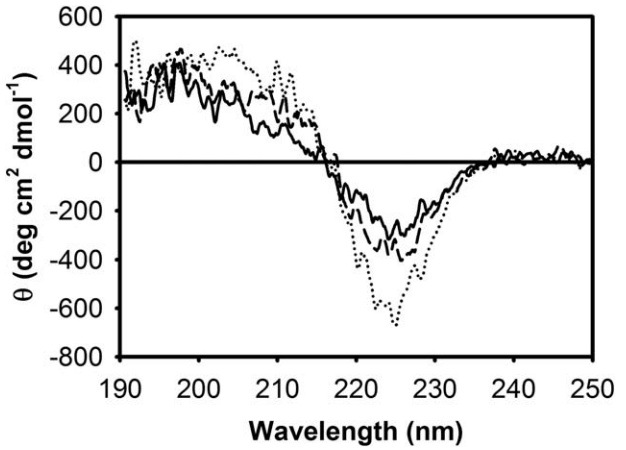

FIGURE 4 Difference far UV-CD spectra obtained after subtracting the spectrum of [K^{108}] 107-115 hLz from that of [$K^{108}W^{111}$] 107-115 hLz at different TFE concentrations: 0 —, 10 – – – and 25%.... v/v.

identified as a consequence of the substitution of Ala by Trp at position 111, namely the major enhancement of the broad negative band at 222 nm and a lesser effect, giving rise to a positive difference near 200 nm. Both signals evolved in a TFE concentration-dependent manner. Interestingly, Trp^{111} was located exactly in the center of the peptide, possibly occupying the most conformationally restricted region. Consistent with this observation was the appearance of a positive difference at around 200 nm, which is indicative of an overall less disordered structure. According to Chakrabartty et al.,[21] an induced negative dichroic signal at around 220 nm could be attributed to the aromatic contribution of Trp in an α-helical environment. In our case, we presume that this band, which was induced by this substitution, represents the location of an indole chromophore in a more structured environment. It is worth mentioning that this characteristic signal near 220 nm was absent in the lead peptide and the other analogs assayed, despite the presence of two Trp residues.

Interestingly, the additional positive charge near the *N* terminus in combination with the extra Trp residue might confer the resultant peptide an appropriate conformation to support enhanced anti-staphylococcal activity. This key feature may improve the interaction with the microbial plasma membrane and its partitioning at the interface. In peptide [$K^{108}W^{111}$] 107-115 hLz, Trp^{111} might represent an additional anchoring element to the lipid membrane, as described for other AMPs.[22]

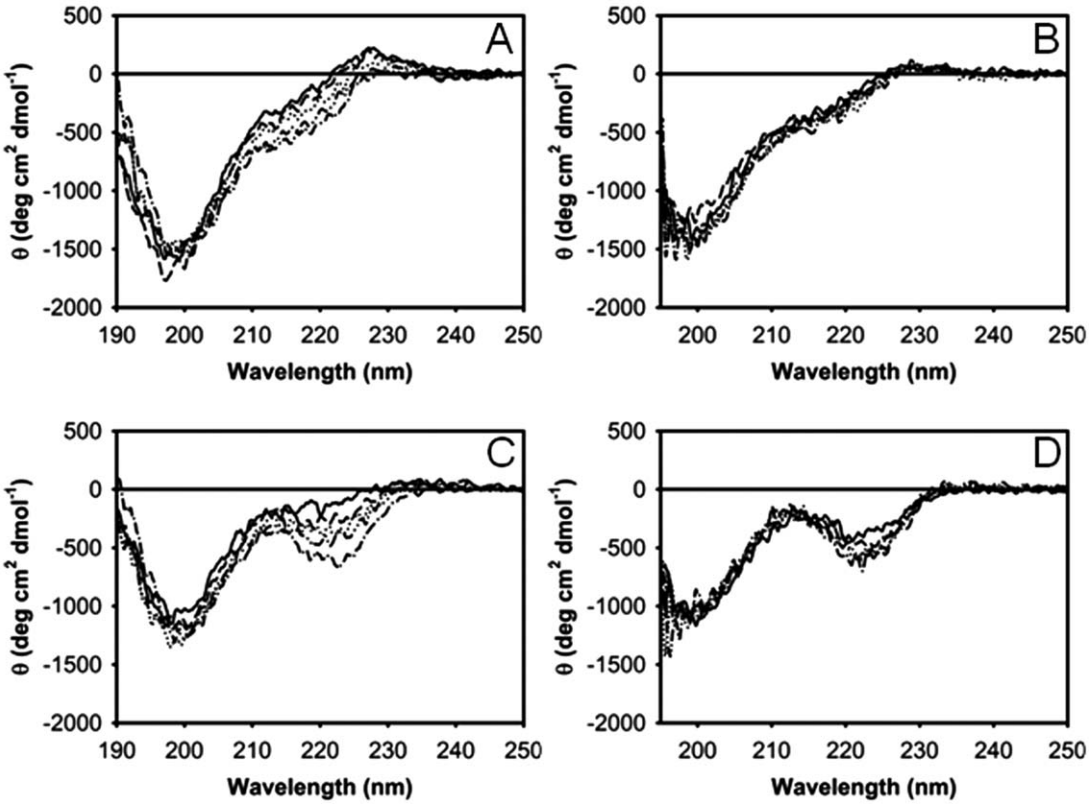

FIGURE 5 Far UV-CD spectra of 107-115 hLz (A, B) and [$K^{108}W^{111}$] 107-115 hLz (C, D) at increasing concentration of DMPC in micellar form. DMPC:peptide molar ratio: 0:1 —, 5:1 – – –, 10:1 ……, 20:1 – . . – and 30:1 – · –. Experiments were carried out in water (A, C) and in PBS (B, D).

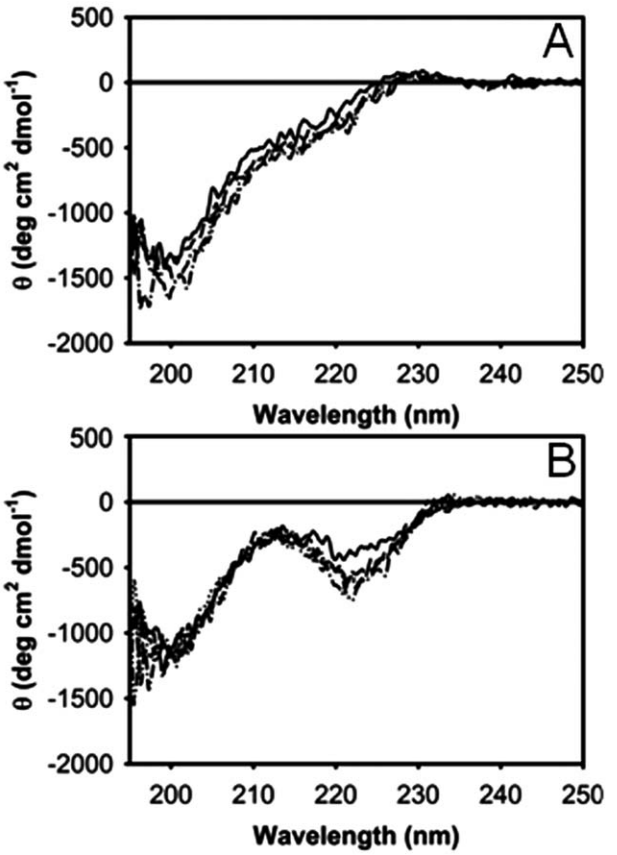

FIGURE 6 Far UV-CD spectra of peptides 107-115 hLz (A) and [K^{108}W^{111}] 107-115 hLz (B) at increasing concentration of DMPC/DMPA micelles in PBS. DMPC:DMPA:peptide molar ratio: 0:0:1 —, 5:1:1 – – –, 10:2:1……, 20:4:1 – · · – and 30:6:1 – · –.

In order to mimic the CAMP interaction with this membrane, we studied the conformational changes of 107-115 hLz and [K^{108}W^{111}] 107-115 hLz upon the addition of lipid:detergent micelles. At this stage, peptides [N^{108}] 107-115 hLz and [K^{108}] 107-115 hLz were discarded from the study because TFE failed to induce any significant conformational change in their structure. Firstly, DMPC:C12E10 micelles (1:2 molar ratio) were incubated with peptides in water and in PBS for CD-spectra record. (Figure 5). For both peptides in water (panels A and C), the electrostatic effect appeared to amplify the conformational changes observed in PBS (panels B and D) (Figure 5). Finally, in order to analyze the influence of a net negative-charged membrane on peptide conformation, thus mimicking the microbial plasma membrane, DMPC:DMPA:C12E10 micelles (1:0.2:2 molar ratio) in PBS were assayed (Figure 6). As observed for TFE, the negative band at 222 nm of peptide [K^{108}W^{111}] 107-115 hLz was altered by exposure to the lipidic environment. For both micelle types, a lipidic concentration-dependent increase in the intensity of this induced band was observed (Figures 5D and 6B). However, no evident conformational change for peptide 107-115 hLz in the presence of either type of micelle was detected (Figures 5B and 6A). This result highlights a distinctive behavior of peptide [K^{108}W^{111}] 107-115 hLz, suggesting that it adopts a more restricted conformation in a microbial plasma membrane-mimicking environment. This feature may facilitate the interaction of the peptide with this barrier, thus potentiating its antimicrobial activity.

A very similar CD-spectral pattern was obtained for indolicidin in the presence of neutral and anionic detergent micelles, DPC and SDS respectively.[23] Indolicidin is a 13-residue Trp-rich CAMP isolated from the granules of bovine neutrophils. The structure of indolicidin was elucidated by NMR in the presence of zwitterionic (DPC) and anionic (SDS) micelles, revealing that the backbone structure in DPC was extended with two half-turns at residues Lys^5 and Trp^8. The charge distribution of indolicidin in DPC micelles shows a hydrophobic core flanked by positively charged regions, located near the two peptide termini, with three of the four charges pointing in a common direction.[23] Of note, [K^{108}W^{111}] 107-115 hLz and indolicidin show high sequence similarity. This trait might represent the convergence of dissimilar peptide sequences into a common active structural motif (+)WXWW(+) (where + is a basic amino acid, see Scheme 2). Interestingly, the residues at which indolicidin describes the two half turns match the two substitutions introduced in 107-115 hLz that lead to [K^{108}W^{111}] 107-115 hLz (shown in red). In this context, we propose that peptide [K^{108}W^{111}] 107-115 hLz forms a U-shaped amphipathic molecule showing a distinct segregation of a hydrophobic core (WVWW) flanked by positively charged hydrophilic regions at both peptide termini (RK and RNR). Further structural determination by NMR will be undertaken to confirm this hypothesis.

A similar pattern was reported by Houghten et al.,[24] who found compound Ac-RRWWCR-NH$_2$ as the most active anti-staphylococcal peptide derived from the screening of a soluble combinatorial library composed by 52 321 400 hexapeptides. Interestingly, this peptide shows sequence resemblance with peptide [K^{108}W^{111}]107-115 hLz, so that their polar/nonpolar residue distribution is comparable. Along these lines, Wang

RKWVWWRNR-NH$_2$	[K^{108}W^{111}] 107-115 hLz
ILPWKWPWWPWRR-NH$_2$	Indolicidin
(+)WXWW(+)	consensus motif

SCHEME 2 Sequence alignment of [K^{108}W^{111}] 107-115 hLz and indolicidin.

RKWVWWRNR	[K^{108}W^{111}] 107-115 hLz
HPLKQYWWRPSI	PW2

SCHEME 3 Sequence alignment of [K^{108}W^{111}] 107-115 hLz and PW2.

et al.[4] proposed that a structural pattern consisting of hydrophobic grooves bordered by basic side-chains has a high membrane perturbation potential.

Tinoco et al.[25] produced some interesting results after screening a phage display library. They reported the consensus sequence WW+ present in peptides with anti-coccidial activity, possibly mediated through membrane permeabilization. Remarkably, this biologically relevant ensemble of amino acid residues is also present in peptide [$K^{108}W^{111}$] 107-115 hLz. Using NMR spectroscopy, they studied the solution structure of the most active peptide of this kind, namely PW2, bound to a micelle interface. The sequences of peptides PW2 and [$K^{108}W^{111}$] 107-115 hLz are aligned in Scheme 3.

Those authors concluded that Trp^7, Trp^8, and Arg^9 are key residues for the interaction with SDS micelles. Additionally, residues Lys^4, Tyr^6, Trp^7, Trp^8, and Arg^9 present the highest chemical shift deviations upon binding to SDS micelles, thus supporting the notion of their key role in micelle-binding. All residues except Tyr^6 are present in peptide [$K^{108}W^{111}$] 107-115 hLz. Furthermore, Lys^4 and Trp^7 match the Ala-substitutions in positions 108 and 111, derived from our screening (shown in red).[9] This finding suggests that this combination confers the resultant peptide the capacity to target and bind to anionic interfaces, such as micelles and microbial plasma membranes, thereby resulting in enhanced anti-staphylococcal activity, as assessed in our previous work.[9]

Overall, our results show that the arrangement in the primary structure of peptide [$K^{108}W^{111}$] 107-115 hLz translates into a more structured conformation in water as well as after induction with TFE or lipidic micelles. Since DMPC/DMPA micelles mimic the bacterial plasma membrane environment more closely, we presume that peptide [$K^{108}W^{111}$] 107-115 hLz adopts an amphipathic conformation, enabling its interaction with the bacterial plasma membrane. This conformation might fit the *Sinking Raft* membrane binding model for short amphipathic CAMPs.[26] This mechanism of action will be further examined by carboxy fluorescein liposome leakage assays.

Fluorescence Spectroscopy

To gain further information about the peptide-micelle interaction, intrinsic fluorescence emission was measured for peptides 107-115 hLz and [$K^{108}W^{111}$] 107-115 hLz in the presence of DMPC or DMPC/DMPA mixed micelles (Figure 7).

Figure 7A shows the fluorescence emission spectra of peptides 107-115 hLz and [$K^{108}W^{111}$] 107-115 hLz in PBS and in the presence of an excess amount of DMPC or DMPC/DMPA micelles. For both peptides, the λ_{max} of the fluorescence emission in buffer matched that of a solvent-exposed Trp: 354 and 356 nm for peptides 107-115 hLz and [$K^{108}W^{111}$] 107-115 hLz,

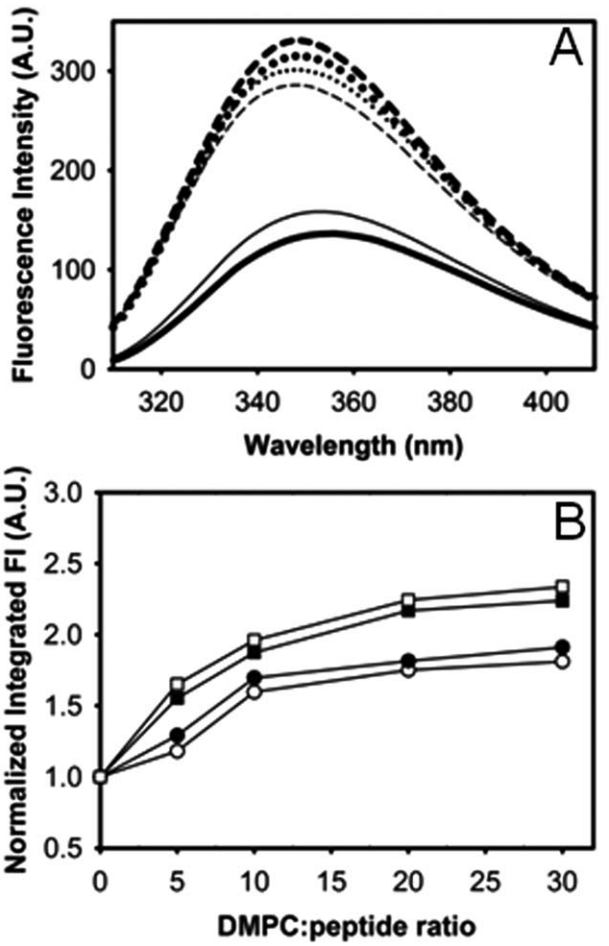

FIGURE 7 A: Fluorescence emission spectra of peptides 107-115 hLz (thin line) and [$K^{108}W^{111}$] 107-115 hLz (bold line) in PBS (—), in the presence of DMPC micelles (30:1, DMPC:peptide ratio, – –) or mixed micelles (30:6:1, DMPC:DMPA:peptide ratio, · · · ·). B: Integrated fluorescence intensity of peptides 107-115 hLz (◯) and [$K^{108}W^{111}$] 107-115 hLz (□) as a function of increasing micelle concentration: DMPC (close symbols) or mixed DMPC/DMPA micelles (open symbols). In each plot the signal is expressed relative to the value in the absence of micelles.

respectively. Upon addition of micelles, the λ_{max} of the two peptides shifted to 348–349 nm, indicating a similar more rigid hydrophobic environment for the fluorophore. This result is consistent with a pronounced interaction with the lipidic interface.

The integrated fluorescence emission intensity of the novel peptide increased to a greater extent than that of the lead peptide, with no significant change attributable to the difference in micelle composition (Figure 7B). One would expect this to happen if the collisional quenching with water is reduced as the Trp side-chains in the peptides switch to a lipidic milieu. It appears that peptide [$K^{108}W^{111}$]107-115 hLz exhibits a higher membrane affinity than the lead peptide, as evidenced by the

somewhat lower DMPC relative excess required to achieve a half-maximal effect.

CONCLUSIONS AND PERSPECTIVES

Our results support the sequential Ala-substitution as a practical technique for the development of improved compounds from lead peptides. In a two-round screening analysis starting from 16 analogs, we found a Trp-rich peptide, with enhanced anti-staphylococcal activity. The polar/nonpolar distribution pattern and the consensus sequence (+)WXWW(+) came out naturally from our screening and are comparable with those of natural AMPs and peptides derived from synthetic or biological combinatorial libraries. The screening strategy that gave rise to this novel CAMP brought about a significant sequence identity with indolicidin (5 out of 9 amino acids), representing the convergence of dissimilar peptide sequences into a common active structural motif. This practical and simple approach might prove valuable for the development of improved analogs from other natural Ala-containing AMPs, such as temporin-Ra and temporin-Rb, recently reported AMPs isolated from frog-skin which have MIC values for *S. aureus* between 22-34 μM.[27] We anticipate that this search method will contribute to reduce capital venture investments for the development of new antimicrobial-drugs from natural sources.

In agreement with other reports,[4,28] net charge, hydrophobicity, amphiphilic balance, and conformation are key features in AMPs development. [$K^{108}W^{111}$]107-115 hLz might conceivably adopt a minimal amphipatic (distorted?) turn conformation upon contact with bacterial membrane-mimicking micelles, adding to this repertoire as a trait that might contribute to its membrane perturbation potential. Because of its comparable activity and small size, this novel CAMP might emerge as a useful starting point for new antimicrobial drug design.

The authors thank Chemo-Romikin SA (Argentina) for the use of their Peptide Synthesizer facilities. NBI, LMC, OC and JMD are researchers of the CONICET (Argentina).

REFERENCES

1. Rivas-Santiago, B.; Serrano, C. J.; Enciso-Moreno, J. A. Infection Immunity 2009, 77, 4690–4695.
2. Menendez, A.; Ferreira, R. B. R.; Brett, F. B. Nat Immunol 2010, 11, 49–50.
3. Brogden, K. A. Nat Rev Microbiol 2005, 3, 238–250.
4. Wang, G.; Li, Y.; Li, X. J Biol Chem 2005, 280, 5803–5811.
5. Papo, N.; Shai, Y. Peptides 2003, 24, 1693–1703.
6. Spellberg, B.; Guidos, R.; Gilbert, D.; Bradley, J.; Boucher, H. W.; Scheld, W. M.; Bartlett, J. G.; Edwards, J. Jr. Clin Infect Dis 2008, 46, 155–164.
7. Williams, K. J.; Bax, R. Curr Opin Investig Drugs 2009, 10, 157–163.
8. Iannucci, N. B.; González, R.; Cascone, O.; Albericio, F. Science against microbial pathogens: communicating current research and technological advances. A. Méndez-Vilas (Ed) 2011, 2, 961–967.
9. González, R.; Albericio, F.; Cascone, O.; Iannucci, N. B. J Pept Sci 2010, 16, 424–429.
10. Ibrahim, H.; Thomas, U.; Pellegrini, A. J Biol Chem 2001, 276, 43767–43774.
11. Papagianni, M. Biotech Adv 2003, 21, 465–499.
12. Iannucci, N. B.; González, R.; Guzmán, F.; Cascone, O.; Albericio, F. Proceedings of the 32nd European Peptide Symposium; Kokotos, G., Constantinou-Kokotou, V., Matsoukas, J., Eds. 2012, 158–159.
13. Iannucci, N. B.; Hollmann, A.; Diaz, M. R.; Cascone, O.; Albericio, F.; Disalvo, E. A. Proceedings of the 22nd American Peptide Symposium. Michal Lebl (Ed) 2011, 294–295.
14. Eisenberg, D.; Weiss, R. M.; Terwilliger, T. C. Proc Natl Acad Sci USA 1984, 81, 140–144.
15. Schmid, F. Protein Structure: A Practical Approach, Creighton, T. E., Ed. IRL, New York, 1989, 251.
16. Roman, E. A.; Rosi, P.; González Lebrero, M. C.; Wuilloud, R.; González Flecha, F. L.; Delfino, J. M.; Santos, J. Proteins 2010, 78, 2757–2768.
17. Pérez-Payá, E.; Houghten, R. A.; Blondelle, S. E. Biochem J 1994, 299, 587–591.
18. Mangoni, M. L.; Carotenuto, A.; Auriemma, L.; Saviello, M. R.; Campiglia, P.; Gomez-Monterrey, I.; Malfi, S.; Marcellini, L.; Barra, D.; Novellino, E.; Grieco, P. J Med Chem 2011, 54, 1298–1307.
19. Grieco, P.; Luca, V.; Auriemma, L.; Carotenuto, A.; Saviello, M. R.; Campiglia, P.; Barra, D.; Novellino, E.; Mangoni, M. L. J Pept Sci. 2011, 17, 358–365.
20. Hong, D.; Hoshino, M.; Kuboi, R.; Goto, Y. J Am Chem Soc 1999, 121, 8427–8433.
21. Chakrabartty, A.; Kortemme, T.; Padmanabhan, S.; Baldwin, R. L. Biochemistry 1993, 32, 5560–5565.
22. Haug, B. E.; Svendsen, J. S. J Pept Sci 2001, 7, 190–196.
23. Rozek, A.; Friedrich, C. L.; Hancock, R. E. W. Biochemistry 2000, 39, 15765–15774.
24. Houghten, R. A.; Pinilla, C.; Blondelle, S. E.; Appel, J. R.; Dooley, C. T.; Cuervo, J. H. Nature 1991, 354, 84–86.
25. Tinoco, L. W.; da Silva, A. Jr.; Leite, A.; Valente, A. P.; Almeida, F. C. L. J Biol Chem 2002, 277, 36351–36356.
26. Chan, D. I.; Prenner, E. J.; Vogel, H. J. Biochimica et Biophysica Acta 2006, 1758, 1184–1202.
27. Asoodeh, A.; Zardini, H. Z.; Chamani, J. J Pept Sci 2012, 18, 10–16.
28. Ifrah, D.; Doisy, X.; Ryge, T. S.; Hansen, P. R. J Pept Sci 2005, 11, 113–121.